

## Sequestration of CO<sub>2</sub> from Domestic Power Generating Set Using Monoethanol Amine (MEA) and Synthesized Mg-Co Metal Oxides

Samuel, J.O.; Olutoye, M.A; Isah, A.G; Adeniyi, O.D and Okafor, J.O.

Department of Chemical Engineering, Federal University of Technology, Minna, Nigeria

### Abstract

A pilot carbon capture plant was used to carry out a base line assessment of CO<sub>2</sub> absorption by MEA at various concentrations with synthesized Mg-Co metal oxides from the exhaust fume of a power generating plant. MEA solution and flue gases run counter currently through a packed column. The metal oxides were prepared and characterized by the following techniques XRD, FTIR, BET, XRF and SEM to gain insights. MEA solution at various concentrations of 10%, 20%, and 30% (v/v) were pumped through the absorption column with glass beads only, then followed by, Magnesium Oxide; Cobalt Oxide and the mixed metal oxides (Magnesium Oxide and Cobalt Oxide), there was an increase in the yield of CO<sub>2</sub> that was captured when the metal oxides were used. However, the best yield of 11.9% was observed when 30 g of magnesium oxide (MgO) with 30% concentration of monoethanol amine solution was used; while the cobalt oxide (CoO) gave the least yield of 5.7% and the mixed metal oxides (MgO - CoO) gave a yield of 9.9%, this yield could be attributed to the contribution from the magnesium oxide (MgO). The yield when only monoethanol amine solution was used was 4.1%. The results showed that the metal oxides enhanced the rate of CO<sub>2</sub> captured and the best performance was observed for magnesium oxide catalyst. The Brunauer – Emmett – Teller (BET) result also revealed that the magnesium oxide (MgO) has the highest pore diameter of (66.9 Å), pore volume of (0.0549 cc/g) and surface area (154 m<sup>2</sup>/g) while the cobalt oxide has the least pore diameter (63.5 Å), pore volume (0.0441 cc/g) and surface area of (124 m<sup>2</sup>/g). Thus, the investigation serves as a green process that could be adopted to reduce global warming and guaranty safe and sustainable environment.

**Keywords:** Carbon capture, Metal oxide, Monoethanol amine, Packed absorption Column, Greenhouse effect.

### Introduction

Sequestration of CO<sub>2</sub> from domestic power generating set using monoethanol amine (MEA) and metal oxides is a technology that can reduce up to 90% of the carbon dioxide (CO<sub>2</sub>) emissions produced from the use of fossil fuels in power generating systems and industrial processes (Socolow and Pacala, 2004). Thus, preventing the carbon dioxide from entering the atmosphere, this will significantly reduce the effect of greenhouse gas emissions to the atmosphere and subsequently reduce global warming (Socolow and Pacala,

2004). While we try to meet up with the demands of the world's future energy and at the same time limit the effect of global warming, designs of power generating plants integrated with a carbon capture system are necessary (Edge *et al.*, 2013).

In 1997 the issue of global warming has been discussed at Kyoto Protocol with the aim of governments ratifying the treaty of "achieving stabilization of greenhouse gas concentrations in the atmosphere at a level that would prevent dangerous anthropogenic interference with the climatic system" The climate change is today

admitted as a problem by almost every scientist, leaders of Nations and concern citizens (Socolow and Pacala, 2004). The major greenhouse gas emitted by human activities is the carbon dioxide which is an end product in all kind of combustions from fossil fuel fired power plants to firewood burning. Carbon in wood, natural gas, oil or coal reacts with oxygen and forms carbon dioxide and water vapour.

Power production is one of the largest contributors to CO<sub>2</sub> emissions through the combustion of coal, oil or natural gas to produce heat and electricity (Socolow and Pacala, 2004). The amount of CO<sub>2</sub> emitted varies with type of fuel and combustion technology available, carbon rich fuels such as coal produce the highest amount of CO<sub>2</sub> while hydrogen rich fuels like natural gas have smaller emissions in comparison (Socolow and Pacala, 2004).

There is an increasing interest in sequestration of CO<sub>2</sub> gas from power generating plant exhaust as a measure to reduce man-made emissions of the greenhouse gas (CO<sub>2</sub>). Several methods have been proposed for CO<sub>2</sub> capture from power plants, both for fossil fuel, natural gas and coal, many of the studies examine the use of monoethanol amine (MEA) as a solvent (Hongyi and Gary, 2001).

Few studies in the literature (Idem *et al.*, 2005) and (Mofarahi *et al.*, 2008) also compared the cost of CO<sub>2</sub> removal using different amine solvents. Chakma *et al.*, (1995) examined the effects of inlet gas composition, feed gas pressure, reboiler energy inputs, and the number of absorber and stripper trays on the cost of CO<sub>2</sub> removal using MEA, it was observed that the cost of amine-based absorption of CO<sub>2</sub>

is relatively high due to high heat duty requirements for the solvent regeneration (Idem *et al.*, 2005) and (Mofarahi *et al.*, 2008). Given this concern, most of the literature focuses on improving the design of amine absorption/desorption processes and their operating conditions to reduce its cost.

This study intends to investigate the use of metal oxide as a substitute or complementary material for sequestration of CO<sub>2</sub> gas from power generating plant exhaust, metal oxides are readily available, require less power and are economical (Dennis *et al.*, 2014).

Based on the characterization of the metal oxide using scanning electron microscope, Brunauer – Emmett – Teller, X-ray fluorescence, Fourier transform infrared, and X-ray diffraction, the synergetic effect of the metal oxide and its activity and the performance.

## Materials and Methods

### Materials

Commercial grade Cobalt (II) Nitrate, Co (NO<sub>3</sub>)<sub>2</sub>·6H<sub>2</sub>O 250 g by weight and 97% purity, Potassium Hydroxide (KOH) Pellets 500 g with 99% purity, Magnesium Nitrate (Mg(NO<sub>3</sub>)<sub>2</sub>·6H<sub>2</sub>O) 500 g with 85% purity, Mono-Ethanolamine (CH<sub>2</sub>(OH).CH<sub>2</sub>.NH<sub>2</sub>) Mwt (61.08) with 99% purity were purchased from Panlac Chemical and Laboratory equipment store at Minna Niger State of Nigeria. These reagents were used without further purification for metal oxidesynthesis



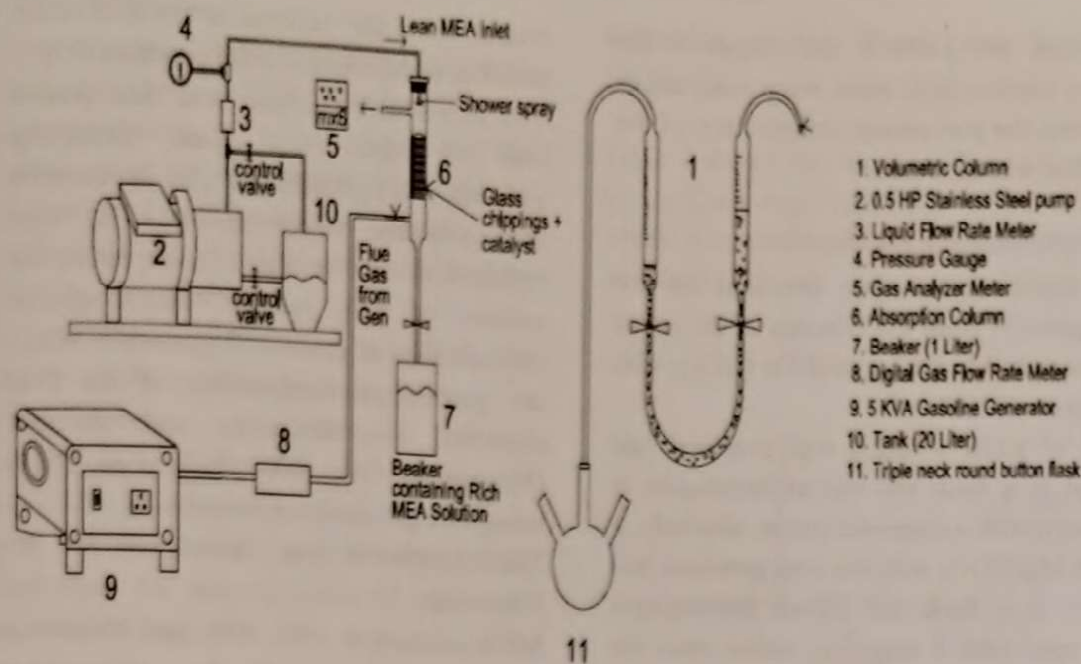


Fig. 1: Experimental setup.

The experimental study is composed of two main parts:

1. Synthesis and characterization of metal oxides.
2. Testing the performance of the synthesized catalyst on fabricated carbon capture pilot plant.

From Fig.1. flue gas from a 5 kva domestic gasoline power generator flows counter currently from the bottom of the column to contact the lean amine solvent (Lean MEA) from the top of the column. The acid gases are absorbed by the amine solvent and the sweet gas leaves the column from the top. The rich amine (Rich MEA) was collected from the bottom of the column in a triple neck round bottom flask connected to a volumetric flask where concentrated hydrochloric acid was used to generate the heat required to release the CO<sub>2</sub> gas trapped in the rich amine, the volume of liquid displaced on the volumetric column indicate the volume of gas released from the rich amine, and the concentration of the

CO<sub>2</sub> gas release was determined using the gas analyser meter (Hongyi and Gary, 2001; Ross *et al.*, 2015).

#### Sample Preparation

##### Preparation of Monoethanol amine (MEA) Solution

The following concentration of MEA were prepared 10%, 20% and 30% (v/v) and gas samples were collected from the exhaust of the domestic power generating set.

##### Gas Sampling

Samplings were carried out with calibrated standard gas analyser (Ibird MX6) to determine the baseline emission data.

**Air:** The air around the power generating plant was analysed to establish a base line data for the air compositions.

**Exhaust fume:** The exhaust fume from the power generating plant was also analysed to determine the base line emission data for the fume compositions which will later be compared with the output gases from the carbon capture system, after the flue gas

treatment, the gases at the output of the carbon capture pilot plant were analysed to ascertain the percentage composition of the CO<sub>2</sub> that was absorbed.

#### Preparation of the metal oxides

The metal oxides were prepared by coprecipitation from the Nitrates of the metal compounds Mg(NO<sub>3</sub>)<sub>2</sub> and Co(NO<sub>3</sub>)<sub>2</sub> with solution of KOH.

2 M of KOH solution was prepared and mixed in a flask and stirred thoroughly at 600 rpm with a magnetic stirrer, similarly, 1 M of Mg(NO<sub>3</sub>)<sub>2</sub> solution was prepared and mixed in a flask and stirred thoroughly at 600 rpm with a magnetic stirrer until the solution becomes homogenous (Olutoye *et al.*, 2011; Olutoye and Hameed, 2010).

To precipitate the Mg(NO<sub>3</sub>)<sub>2</sub>, 100 ml of an aqueous KOH solution was added to 100 ml solution of the Mg(NO<sub>3</sub>)<sub>2</sub> to get the corresponding magnesium oxide which is then mixed in a flask and stirred thoroughly at 600 rpm with a magnetic stirrer.

The corresponding mixtures were then stirred continuously for 6 h until the solution is homogenized, the solution is then filtered and dried at oven temperature of 85 °C for 24 h. which was followed by calcination at a temperature of 460 °C for 4 h (Olutoye *et al.*, 2011; Olutoye and Hameed, 2010).

Similar procedure was followed precipitating the solution of (Co(NO<sub>3</sub>)<sub>2</sub>) to get the corresponding Cobalt Oxide.

The carbon capture system is divided into two sections. One is the CO<sub>2</sub> capture part and the other is the CO<sub>2</sub> release part.

The absorption column is packed with metal oxides (magnesium and cobalt oxides) the lean MEA solution and the flue gas run through the column in a counter-current flow, the inlet flow rate of both the MEA solution and flue gas are set. The liquid

output from the column is the rich MEA solution which contains the captured CO<sub>2</sub>.

The rich MEA solution was then poured into a triple neck flask containing concentrated hydrochloric acid the reaction is exothermic which generate the heat required to release the CO<sub>2</sub> captured, the volume of CO<sub>2</sub> release was monitored through a set of graduated glassware. While the percentage composition of the CO<sub>2</sub> captured was determine and recorded (Hongyi and Gary, 2001; Ross *et al.*, 2015) using flue gas analyser meter.

The experiment was carried out for the following:

- MEA solution at 10%, 20%, and 30% (v/v) concentration through the pilot plant absorption column with glass packing only.
- MEA solution at 10%, 20%, and 30% (v/v) concentration through the pilot plant absorption column with Magnesium Oxide at 10 g, 20 g and 30 g respectively.
- MEA solution at 10%, 20%, and 30% (v/v) concentration through the absorption column with Cobalt Oxide at 10 g, 20 g and 30 g respectively.
- MEA solution at 10%, 20%, and 30% (v/v) concentration through the absorption column with the mixed oxides (magnesium oxide and cobalt oxide) at 10 g, 20 g and 30 g respectively.

The experiment was repeated for steps 2 to 4 with different quantity of magnesium oxide, cobalt oxide and the mixed oxides (magnesium oxide and cobalt oxide) as described above.

The composition with the best CO<sub>2</sub> captured was determined and recorded (Hongyi and Gary, 2001; Ross *et al.*, 2015).



### Characterization

Synthesis and characterization of MgO, CoO and MgO – CoO mixed oxides for carbon capture, the metal oxides and the mixed metal oxides were synthesized by co-precipitation technique and the synthesized metal oxides were analysed by the following methods:

- X-ray diffraction (XRD) for detection of crystalline phases,
- Fourier Transform Infrared Spectroscopy (FTIR) for determination of functional group
- Brunauer – Emmett – Teller (BET) Technique for determination of pore size and surface area
- Scanning Electron Microscopy (SEM) for morphology
- X-Ray Florescence (XRF) for composition analysis

**Table 1:** X-ray Diffraction Angles for Metal Oxides

S/No	Metal Oxides	Diffraction Angles for Strongest 3 Peaks (Degree)
1	Magnesium Oxide (MgO)	18.3, 24.1 and 47.6
2	Cobalt Oxide (CoO)	24.1, 25.0, and 25.5
3	Mixed Oxide (MgO - CoO)	24.1, 25.0, and 25.4

### Results and discussion

#### X-ray Diffraction (XRD) Data Analysis

The characterization of crystal structure and determination of crystallographic parameters of the metal oxides were performed by XRD analysis. Metal oxides with three different compositions were prepared by precipitation method and their X-ray diffraction patterns were recorded, the XRD pattern of CoO, MgO and CoO – MgO are depicted in Fig. 2 – 4 which indicate the crystalline nature and the peaks at scattering angles ( $2\theta$ ) with the following

diffraction angles (Figen and Baykara, 2012).

Table 1 shows the strongest three (3) peaks for the CoO, MgO and CoO – MgO oxides, which was also represented in the plots as seen in (Fig. 2 - 4).

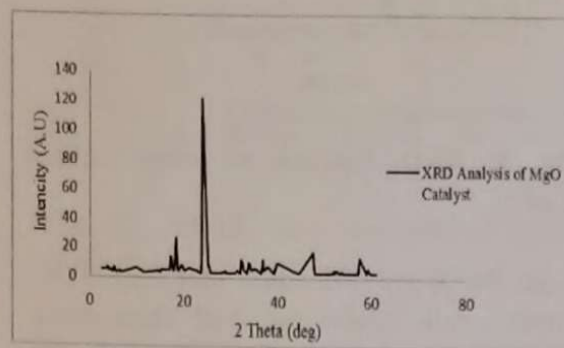


**Fig. 2:** XRD Analysis of magnesium oxide (MgO).

From the X-ray diffraction plot (Fig. 2) of magnesium oxide (MgO) the sharp peak occurs at point  $24.1^\circ$  on the  $2\theta$  scattering angle axis this corresponds to the face centre cubic crystalline structure of magnesium oxide (Figen and Baykara, 2012).

Other peaks with low intensity were also seen, this could be attributed to a long range order induced by the very regular arrangement of the pores which lead to new phase and structure of magnesium oxide that was developed (Margandan, *et al.*, 2010).

Similar work was reported by Cimi, (2014) where Synthesis, Characterization and catalytic activity of nanocrystalline ceria modified with zirconia were looked into, it was observed that for mesoporous materials, reflections were observed in X-ray powder patterns at low  $2\theta$  angles ( $0.5 < 2\theta < 100$ ). These reflexes are due to the long range order induced by the very

regular arrangement of the poresas observed in the XRD plots (Cimi, 2014).

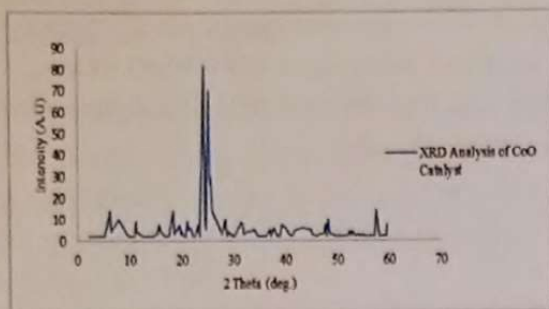


**Fig. 3:** XRD Analysis of cobalt oxides (CoO).

From the X-ray diffraction plot (Fig. 3) of cobalt oxide (CoO) the dual sharp peak occurs at point 24 ° and 25° on the 2θ scattering angle axis this corresponds to the overlapping crystalline phase in the hexagonal closed packed crystalline structure of cobalt oxide.

Bernard and Motin, (2012) reported that cobalt oxide has different sizes of ions in its valence state (Co<sup>4+</sup>, Co<sup>3+</sup>, and Co<sup>2+</sup>) which are not similar, they influence the lattice energy, which in turn affects the physical and structural properties of the crystals this could be attributed to the unstable pattern of the new crystalline structure formed, thus the dual sharp peak observed (Bernard and Motin, 2012).

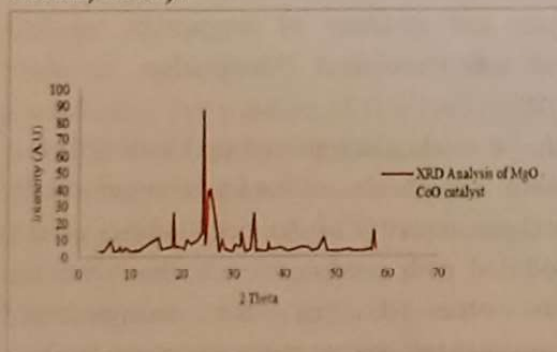


**Fig. 4:** XRD Analysis of mixed magnesium and cobalt oxides (MgO – CoO).

From the X-ray diffraction plot (Fig. 4) of mixed magnesium and cobalt oxides (MgO – CoO), it was observed that there was a drop in the intensity of the dual sharp peak which occurs at point 24 ° and 25° on the 2θ scattering angle axis. This can be attributed to the combinatorial effect of the two metal oxides which gives rise to new phase and a new structure developed as a result of a synergetic effect (Yasuo *et al.*, 1998).

Yasuo *et al.* (1998) reported that when cobalt ion increases in MgO - CoO the solid solution becomes distorted around cobalt. This agrees with the studies carried out by Bernard and Motin, (2012), which state that cobalt oxide has different sizes of ions in its valence state (Co<sup>4+</sup>, Co<sup>3+</sup>, and Co<sup>2+</sup>) which are not similar, they influence the lattice energy, which in turn affects the physical and structural properties of the crystals this could be attributed to the unstable pattern of the new crystalline structure that was formed (Bernard and Motin, 2012).

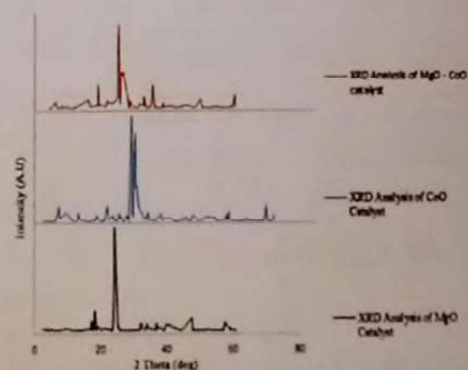


**Fig. 5:** XRD Spectra of metal oxides (MgO, CoO and MgO – CoO).

#### Fourier Transform Infrared Spectroscopy (FT-IR) Data Analysis.

The FT-IR Spectra of the MgO, CoO and CoO – MgO samples are represented in the Fig. (6 -8)

Magnesium Oxide (MgO):



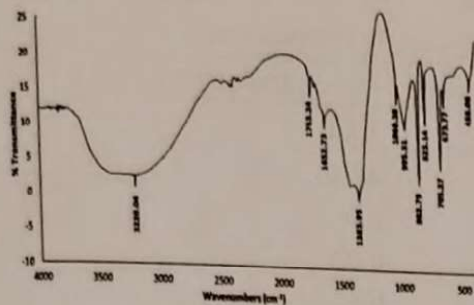


Fig. 6: FT-IR data analysis of Magnesium oxide (MgO).

From the FT-IR plot (Fig. 6), the functional group revealed by the peaks showed that magnesium oxide follows a distinct band at (825), (883), (1060) and (3220)  $\text{cm}^{-1}$  (Foil and Charles, 1952) which appeared in the pure magnesium oxide sample and corresponds to a stretching vibration of the MgO (Rajesh *et al.*, 2013).

*Cobalt Oxide (CoO):*

From the FT-IR plot (Fig. 7), the functional group revealed by the peaks showed that cobalt oxide follows a distinct band at (507) and (3420)  $\text{cm}^{-1}$  which appeared in the impure cobalt oxide and corresponds to a stretching vibration of the cobalt oxide (CoO) (Foil and Charles, 1952).

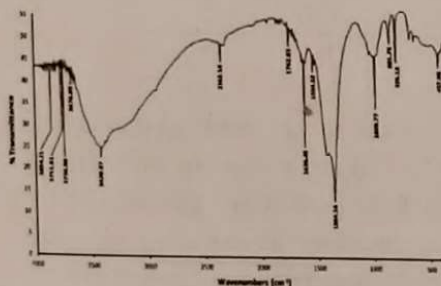


Fig. 7: FT-IR data analysis of Cobalt oxide (CoO)

*Mixed magnesium and cobalt (MgO - CoO) Oxides:*

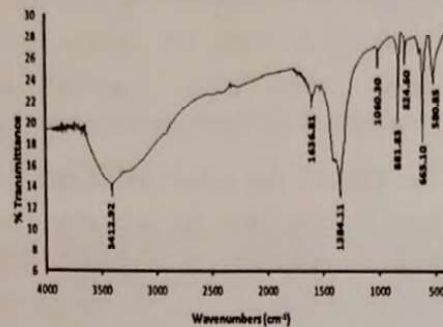


Fig. 8: FT-IR data analysis of mixed oxides (MgO – CoO).

From the FT-IR plot (Fig. 8), the functional group revealed by the peaks showed the following distinct bands at (3410), (1640), (580), (665), (652), (1060), (882) and (885)  $\text{cm}^{-1}$  which appeared in the impure mixed metal oxides sample it corresponds to the stretching vibration of the CoO – MgO. It was observed that the distinct band that occur at (885) and (1060)  $\text{cm}^{-1}$  came as a contribution from the magnesium oxide while the band that occur at (3410)  $\text{cm}^{-1}$  was from the cobalt oxide.

The FT-IR Spectra obtained were in agreement with results reported in the study carried out by Chih-Wei (2011) on Characterization of cobalt oxides studied by FT-IR, Raman, TPR and TG-MS (Chih-Wei *et al.*, 2011).

*Brunauer – Emmett – Teller (BET) Data Analysis:*

From the BET results, the pore size/diameter (nm) and surface area ( $\text{m}^2\text{g}^{-1}$ ) are tabulated in Table 2 as follows:

**Table 2:** BET Results for Surface area pore size Distribution

Metal Oxide	Pore Volume Data (cc/g)	Surface Area (m <sup>2</sup> g <sup>-1</sup> )	Pore diameter (Å)
MgO	0.0549	154	66.9
CoO	0.0441	124	63.5
(MgO-CoO)	0.0500	141	68.7

From the Table 2 the cobalt oxide has the least pore volume and surface area this could be attributed to the unstable pattern of the new crystalline structure formed as reported by Bernard and Motin, 2012 that cobalt oxide has different sizes of ions in its valence state (Co<sup>4+</sup>, Co<sup>3+</sup>, and Co<sup>2+</sup>) which are not similar, they influence the lattice energy, which in turn affects the physical and structural properties of the crystals (Bernard and Motin, 2012).

The mixed oxides (MgO – CoO) was observed to have a better pore volume and surface area result than the cobalt oxide (CoO) this can be attributed to the combinatorial effect of the two metal oxides (Yasuo *et al.*, 1998).

*X-ray Fluorescence (XRF) for Composition Analysis*

From Table 3, it was observed that magnesium oxide (MgO) and potassium oxide (K<sub>2</sub>O) were in high proportion, this should be expected because the magnesium oxide was prepared by precipitation of magnesium nitrate solution with potassium hydroxide solution (Olutoye, and Hameed, 2010). From the X-ray Fluorescence (XRF) composition analysis, the results for each composition was tabulated as follows:

**Table 3:** XRF Data for magnesium oxide (MgO) sample composition

Compound	Concentration (%)
SO <sub>3</sub>	5.60
K <sub>2</sub> O	45.50
TiO <sub>2</sub>	0.06
MnO	0.02
Fe <sub>2</sub> O <sub>3</sub>	0.42
Co <sub>3</sub> O <sub>4</sub>	0.01
CuO	0.04
ZnO	0.02
MgO	42.25
MoO	1.40
Ag <sub>2</sub> O	4.32
Eu <sub>2</sub> O	0.12
Er <sub>2</sub> O <sub>3</sub>	0.03
Re <sub>2</sub> O <sub>7</sub>	0.21
	100

**Table 4:** XRF Data for cobalt oxide (CoO) sample composition

Compound	Concentration (%)
P <sub>2</sub> O <sub>5</sub>	0.13
SO <sub>3</sub>	0.48
K <sub>2</sub> O	32.77
Fe <sub>2</sub> O <sub>3</sub>	0.09
Co <sub>3</sub> O <sub>4</sub>	63.78
GeO <sub>2</sub>	0.29
Ag <sub>2</sub> O	2.19
Nd <sub>2</sub> O <sub>3</sub>	0.07
Eu <sub>2</sub> O <sub>3</sub>	0.20
	100

From Table 4 it was observed that cobalt oxide (Co<sub>3</sub>O<sub>4</sub>) and potassium oxide (K<sub>2</sub>O) were in high proportion, this should be expected because the cobalt oxide was prepared by precipitation of cobalt nitrate solution with potassium hydroxide solution (Olutoye and Hameed, 2010).



**Table 5:** XRF Data for mixed oxides (MgO – CoO) sample composition

Compound	Concentration (%)
SiO <sub>2</sub>	14.60
SO <sub>3</sub>	3.00
K <sub>2</sub> O	44.52
MnO	0.01
Fe <sub>2</sub> O <sub>3</sub>	0.07
Co <sub>3</sub> O <sub>4</sub>	20.45
Nd <sub>2</sub> O <sub>3</sub>	0.05
Eu <sub>2</sub> O <sub>3</sub>	0.10
MgO	17.20
100	

From Table 5, it was observed that cobalt oxide (Co<sub>3</sub>O<sub>4</sub>), magnesium oxide (MgO) and potassium oxide (K<sub>2</sub>O) were in high proportion, this should be expected because the mixed oxides (MgO – CoO) was prepared by co-precipitation of cobalt and magnesium oxide solution with potassium hydroxide solution (Olutoye and Hameed, 2010).

**Table 6** XRF Data for total metal oxides composition

Catalyst	CoO (wt %)	MgO (wt %)
MgO	0	42
CoO	63.78	0
MgO - CoO	20.45	17.2

The summary of the quantitative X-ray fluoroscopy (XRF) analysis results are given in Table 6. The results indicated that the theoretical preparation of the metal oxides was compatible with the X-ray fluoroscopy (XRF) analysis results.

#### Scanning Electron Microscopy (SEM)

From the Scanning Electron Microscopy (SEM) images of the synthesized metal oxides it was observed that the metal oxides adopted an irregular morphology with

different sizes and particles, the images revealed the porous nature of the metal oxides with a well develop pores, from Fig. 9 it was observed that the magnesium oxide (MgO) shows a larger pore size than the other oxides and have large number of aggregate constituent particles agglomerated together on its surface (Hyun *et al.*, 2013).

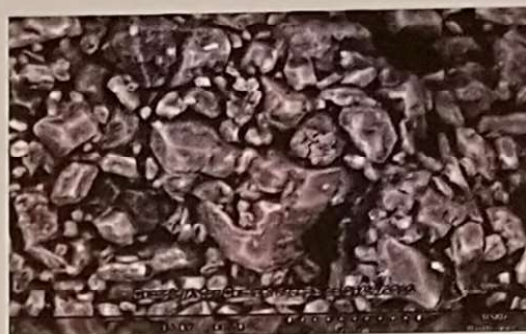


**Fig. 9:** SEM Image of magnesium oxide

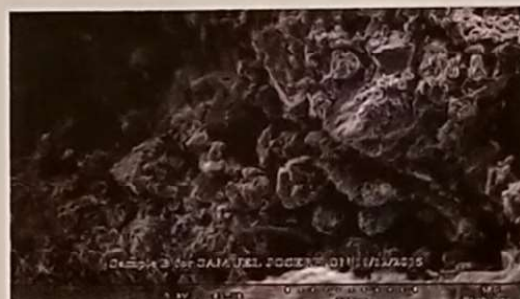


**Fig. 10:** SEM Image of cobalt oxide



**Fig. 11:** SEM Image of mixed oxides (MgO – CoO)

From Fig. 10 it was observed that the SEM image of cobalt oxide sample has the less homogeneous structure in terms of particle size and the aggregate constituent of particles agglomerated together on its surface this is in agreement with the studies carried out by Bernard and Motin (2012) that cobalt oxide has different sizes of ions in its valence state (Co<sup>4+</sup>, Co<sup>3+</sup>, and Co<sup>2+</sup>) which are not similar, they influence the lattice energy, which in turn affects the physical and structural properties of the crystals (Bernard and Motin, 2012). Moreover, from Fig. 11 the image clearly show that the combination of the magnesium oxide and cobalt oxide improves dispersion in the metallic layer of MgO – CoO surface this is as a result of the synergetic effect of MgO over the cobalt oxide this is in agreement with the studies carried out by Figen and Baykara (2012).

*Monoethanol amine (MEA) Run at Different Percentage Concentration only.*

CO<sub>2</sub> percentage conversion plots:

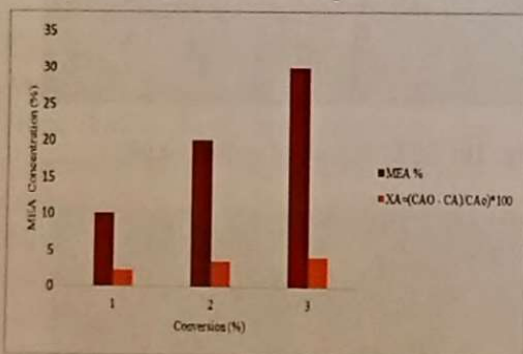


**Fig. 12:** Case (1) Monoethanol amine (MEA) run at different percentage concentrations only.

*Monoethanol amine Run at Different Percentage Concentrations with Metal Oxides.*

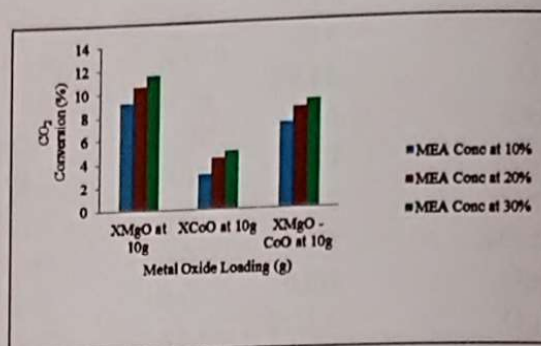


**Fig. 13:** Case (2) Magnesium, cobalt and the mixed oxides at 10 g with different percentage concentrations of MEA

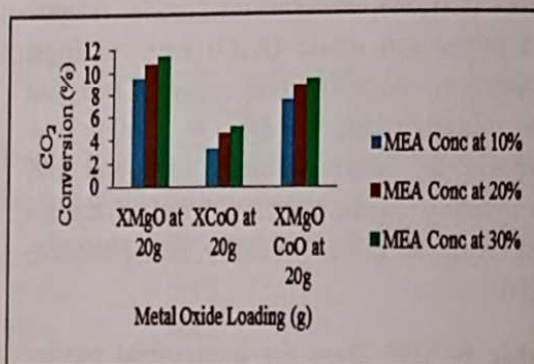


**Fig. 14:** Case (3) Magnesium, cobalt and the mixed oxides at 20 g with different percentage concentrations of MEA

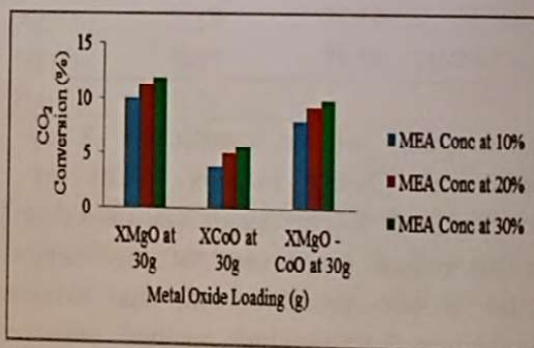


**Fig. 15:** Case (4) Magnesium, cobalt and the mixed oxides at 30 g with different percentage concentrations of MEA



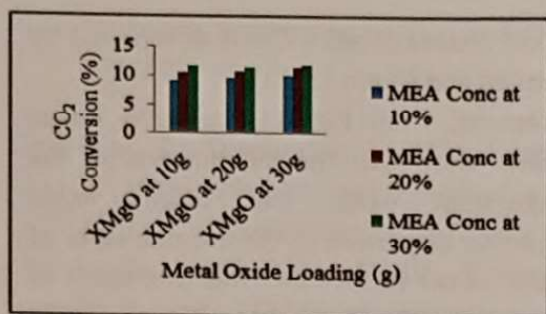


**Fig. 16:** Case (5) Magnesium oxides at 10 g, 20 g, and 30 g with different percentage concentrations of MEA

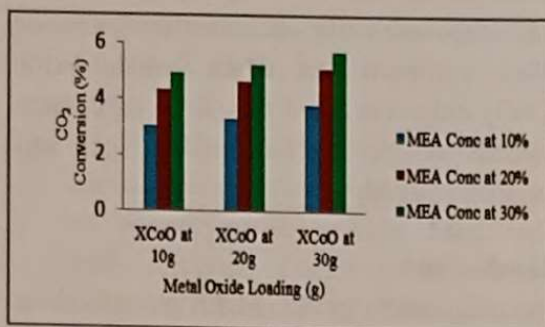


**Fig. 17:** Case (6) Cobalt oxide at 10 g, 20 g, and 30 g with different percentage concentrations of MEA

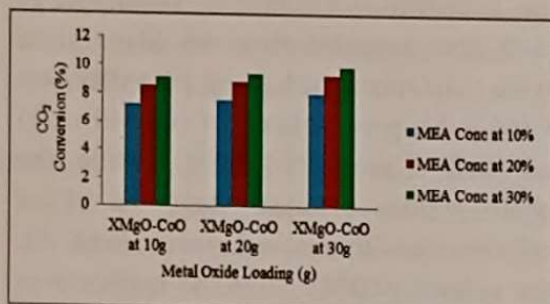


**Fig. 18:** Magnesium and cobalt (MgO – CoO) mixed oxides at 10 g, 20 g, and 30 g with different percentage concentrations of MEA

The results obtained from the experimental work revealed that within the limit of experimental error, there was an increase in the yield of CO<sub>2</sub>, that was captured when the metal oxides were used than when only monoethanol amine was used, as shown in Figs. 13 - 15 and 12 respectively.

Where it was also observed that the higher the concentration of the monoethanol amine

and the metal oxides loading the better the capture performance as shown in Figs 13 - 15, in all cases the highest of the sequestration occur at the top of the CO<sub>2</sub> conversion axis on the plots.

To achieve a significant percentage reduction of CO<sub>2</sub> gas sequestered from the flue gas the experiment has to be run several times, and the higher the numbers of the runs the higher the percentage of CO<sub>2</sub> sequestered. Rose *et al.* (2015) reported 69% reduction in CO<sub>2</sub> at 48 runs (Rose *et al.*, 2015).

In this study, however, the best yield was observed when 30 g of Magnesium Oxide (MgO) and 30% concentration of monoethanol amine solution was used, it gives a yield of 11.9% as shown in Figure 16, while the mixed magnesium oxide and cobalt oxide (MgO - CoO) gives a yield of 9.9% in a ratio of 1:1 for MgO to CoO combination as shown in Fig. 18 the Cobalt Oxide (CoO) gives a yield of 5.7% as shown in Fig. 17 while when only MEA solution was used it gives the least yield of 4.1% as shown in Fig. 12.

The high yield observed when magnesium oxide (MgO) was used could be attributed to its good surface morphology, higher pore diameter of 66.9 Å, pore volume of 0.0549 cc/g and surface area of 154 m<sup>2</sup>/g as presented in Table 2.

It was also observed from Fig. 9 that magnesium oxide (MgO) have a large number of aggregate constituent particles agglomerated together on its surface, thus this makes the magnesium oxide a good material for the CO<sub>2</sub> absorption when compared to cobalt oxide (CoO) and the mixed oxides (CoO – MgO) this is in agreement with the studies carried out by Rajesh (2013) that revealed that the magnesium oxide particle size increase with



increase in the sintering time (Rajesh *et al.*, 2013).

From Table 2, the cobalt oxide has the least pore volume and surface area of 63.5 Å, a pore volume of 0.0441 cc/g and a surface area 124 m<sup>2</sup>/g, this could be attributed to the unstable pattern of the new crystalline structure formed as reported by Bernard and Motin, (2012) that cobalt oxide has different sizes of ions in its valence state (Co<sup>4+</sup>, Co<sup>3+</sup>, and Co<sup>2+</sup>) which are not similar, they influence the lattice energy, which in turn affects the physical and structural properties of the crystals (Bernard and Motin, 2012). This is in agreement with the studies carried out by Yasuo *et al.* (1998).

It was also observed from Fig. 10 that the SEM image of cobalt oxide sample has the less homogeneous structure in terms of particle size and the aggregate constituent of particles agglomerated together on its surface, this is in agreement with the studies carried out by (Bernard and Motin, 2012).

From the results obtained it can be concluded that the cobalt oxide (CoO) is not a good material for the CO<sub>2</sub> absorption when compared to magnesium oxide (MgO).

From Table 2, the mixed oxides (MgO – CoO) was observed to have a better pore volume of 0.0500 cc/g and a surface area 141 m<sup>2</sup>/g, this can be attributed to the combinatorial effect of the two metal oxides (Yasuo *et al.*, 1998).

Yasuo *et al.* (1998) reported that when cobalt ion increases in MgO - CoO the solid solution becomes distorted around cobalt, this implies that cobalt oxide played an inhibitory role on the performance of the

mixed oxides (MgO - CoO) as reported by Bernard and Motin (2012).

Moreover, from Fig. 11 the SEM image clearly show that the combination of the magnesium oxide and cobalt oxide improves dispersion in the metallic layer of MgO – CoO surface this was as a result of the synergetic effect of magnesium oxide (MgO) over the cobalt oxide (CoO).

The contributions of the magnesium oxide (MgO) in the mixed catalyst (MgO - CoO) was responsible for its better performance when compared to when cobalt oxide (CoO) only was used this is in agreement with the studies carried out by Figen and Baykara (2012).

### Conclusion

The magnesium oxide (MgO) gave the best performance in comparison with cobalt oxide and the mixed magnesium and cobalt oxide (MgO – CoO).

The Brunauer – Emmett – Teller (BET) result also revealed that the Magnesium Oxide (MgO) has the highest pore diameter of (66.9 Å), pore volume of (0.0549 cc/g) and surface area (154 m<sup>2</sup>/g), while the cobalt oxide catalyst has the least performance with a pore diameter (63.5 Å), pore volume (0.0441 cc/g) and surface area of (124 m<sup>2</sup>/g).

### References

- Bernard, R. and Motin, S.M.D. (2012). Cobalt Oxides: From Crystal Chemistry to Physics, First Edition. Wiley-VCH Verlag GmbH & Co. KGaA Germany 3.
- Chakma, A.; Mehrotra, A. K. and Nielsen, B. (1995). Comparison of chemical solvents for mitigating CO<sub>2</sub> emissions from coal-fired power plants. Heat



- Recovery Systems and CHP, Vol.15, 231-240.
- Chih-Wei, T.; Tsann-Yan, L.; Wen-Yueh, Y.; Chen-Bin, W. and Shu-Hua, C. (2011). Characterization of cobalt oxides studied by FT-IR, Raman, TPR and TG-MS. Department of Applied Chemistry & Materials Science, Chung Cheng Institute of Technology, National Defence University, Tahsi, Taoyuan, 33509, Taiwan, R. O. C., 1-9.
- Cimi A. D. (2014). Synthesis, Characterization and catalytic activity of nanocrystalline Ceria Modified with Zirconia. Thesis submitted to Cochin University of Science and Technology for the degree of Doctor of Philosophy in Chemistry Under the Faculty of Science Department of applied Chemistry Cochin University of Science and Technology Cochin-682 022, Kerala, India. 48.
- Dennis, Y.C.; Leung, G. C. and Mercedes M. M. (2014). An overview of current status of carbon dioxide capture and storage technologies. Department of Mechanical Engineering, The University of Hong Kong, Hong Kong. Vol. 39, 426-443
- Edge, P. J.; Heggs, P.J.; Pourkashanian, M. and Stephenson, P.L. (2013). Integrated fluid dynamics - process modelling of a coal - fired powerplant with carbon capture a Centre for Computational Fluid Dynamics, University of Leeds, Leeds LS2 9JT, UK. Applied Thermal Engineering Vol. 1, No. 60, 242 - 250.
- Figen, H.E. and Baykara, S.Z. (2012). Preparation and Characterization of Co-Mo/-Al<sub>2</sub>O<sub>3</sub>, Ni-Mo/-Al<sub>2</sub>O<sub>3</sub> and (Co/Ni)-Mo/-Al<sub>2</sub>O<sub>3</sub> Metal Oxides by Sol-Gel Process. Chemical Engineering Department, Yildiz. Technical University, Topkapi, Istanbul 34210, Turkey. *ACTA PHYSICA POLONICA A*. Vol. 121, 1-3
- Foil, A. M. and Charles, H.W. (1952). Infrared Spectra and Characteristic Frequencies of Inorganic Ions Their Use in Qualitative Analysis. Department of Research in Chemical Physics, Mellon Institute, Pittsburgh 13, Pa. U.S.A. Vol. 24, No 8, 2-6.
- Hongyi, D. and Gary, T. R. (2001). CO<sub>2</sub> Absorption Rate and Solubility in Monoethanol amine /Piperazine /Water. The University of Texas at Austin Department of Chemical Engineering Austin, Texas 78712. Prepared for presentation at the First National Conference on Carbon Sequestration. Washington, DC, 1-17.
- Hyun, T. J.; Eui, M. J.; Sang H.P. and Pushparaj, H. (2013). Synthesis and Characterization of CoO - ZnO Catalyst System for Selective CO Oxidation. Department of Chemical Engineering, Hanseo University, Seosan-si 356-706, South Korea International Journal of Control and Automation Vol. 8, No 6, 31-40. <http://dx.doi.org/10.14257/ijca.2013.6.04>

*Sequestration of CO<sub>2</sub> from Domestic Power Generating Set Using Monoethanol Amine (MEA) and Synthesized Mg-CO Metal Oxides*

- Idem, R., Wilson, M.; Tontiwachwuthikul, P.; Chakma, A.; Veawab, A. and Aroonwilas, A. (2005). Pilot Plant Studies of the CO<sub>2</sub> Capture Performance of Aqueous MEA and Mixed MEA/MDEA Solvents at the University of Regina CO<sub>2</sub> Capture Technology Development Plant and the Boundary Dam CO<sub>2</sub> Capture Demonstration Plant. *Industrial & Engineering Chemistry Research*, Vol. 1, No. 45, 2414-2420.
- Margandan, B.; Pushparaj, H.; Mani, G.; Peng, M. M. and Hyun, T. J. (2010). A direct synthesis of mesoporous carbon supported MgO sorbent for CO<sub>2</sub> Capture, Chemical Engineering Department, Hansoo University, Seosan 360 – 706 South Korea, 1 – 6.
- Mofarahi, M.; Khojasteh, Y.; Khaledi, H. and Farahnak, A. (2008). Design of CO<sub>2</sub> absorption plant for recovery of CO<sub>2</sub> from flue gases of gas turbine. *Energy*, Vol. 1, No. 33, 1311-1319.
- Olutoye, M.A.; Lee, S.C. and Hameed, B.H. (2011). Synthesis of fatty acid methyl ester from palm oil (*Elaeisguineensis*) with  $K_y(MgCa)_{2x}O_3$  as heterogeneous catalyst. School of Chemical Engineering, Engineering Campus, University Sains Malaysia, 14300 NibongTebal, Penang, Malasia. *Bioresource Technology*. Vol. 1, No. 102, 10777-10783.
- Olutoye, M.A. and Hameed, B.H. (2010). Transesterification of palm oil on  $K_yMg_{1-x}Zn_x + xO_3$  Catalyst: Effect of Mg-Zn Interaction. School of Chemical Engineering, Engineering Campus, University Sains Malaysia, 14300 NibongTebal, Penang, Malasia. *Fuel Processing Technology* Vol. 1, No. 91, 653-659.
- Rajesh K.; Ashwani, S. and Nawal K. (2013). Preparation and Characterization of MgO Nanoparticles by Co-Precipitation Method. *International Journal of Engineering, Applied and Management Sciences Paradigms*, Vol. 07, Issue 01, 1-5.
- Ross, E. D.; Gary, T. R. and Frank, S. (2015). CO<sub>2</sub> capture performance of a monoethanolamine pilot plant. Department of Chemical Engineering, The University of Texas at Austin TX 78758, USA, 1 – 6.
- Socolow, R and Pacala, S. (2004). Stabilization Wedges: Solving the Climate Problem for the Next 50 Years with Current Technologies. *Science*. Vol. 305, No. 5686, 968 – 972.
- Yasuo, I.; Kenzo, O. and Ken-ichi, A. (1998). Characterization of active site on cobalt – magnesium oxide by X-Ray Absorption fine structure spectroscopy. Department of Environmental Chemistry and Engineering, Institute of Technology Yokohama, Japan, 726.